J. Fluid Mech. (2005), *vol.* 537, *pp.* 255–270.
doi:10.1017/S0022112005005252 Printed in the United Kingdom

Planform selection in Rayleigh–Bénard convection between finite slabs

By B. HOLMEDAL[1], M. TVEITEREID[2] AND E. PALM[3]

[1]Department of Materials Technology, Norwegian University of Science and Technology, N-7491 Trondheim, Norway

[2]Agder College, N-4876 Grimstad, Norway

[3]Mechanics Division, Department of Mathematics, University of Oslo, Blindern, N-0316, Norway

(Received 25 May 2003 and in revised form 7 March 2005)

Thermal convection in a thin horizontal fluid layer enclosed between two rigid slabs of arbitrary thicknesses and conductivities has been investigated. We have found a mathematical transformation between this problem and the problem of the upper and lower slabs being interchanged. A weakly nonlinear expansion has been applied to reduce the governing equations to a set of Landau equations. Their extremum principle combined with an analytical solution for the case of insulating slabs has been used to prove that rhombuses and rolls are the only stable solutions. Hexagons, quasi-patterns and any solution involving higher numbers of modes, are proved to be unstable. Stability regions of rolls and rhombuses have been found numerically for a wide range of slab conductivities and thicknesses. The wavenumber selection has been investigated by studying two coupled Ginzburg–Landau equations. Earlier stability analyses of Proctor's equation valid for the limit of poorly conducting slabs has revealed that the wavenumbers of squares, i.e. rhombuses with orthogonal wave vectors, are restricted by a zigzag instability and by a truly three-dimensional instability. We show here that the wavenumber selection for more general cases with finite conductivities and thicknesses of the slabs are always restricted by the same types of instability. In addition, we show how the stability and wavenumber selection of another solution of the Ginzburg–Landau equations, the undulated rolls, is restricted by a cross-roll instability.

1. Introduction

During the last century a large number of investigations of Rayleigh–Bénard convection have been carried out since the pioneering studies of Bénard (1900), and Rayleigh (1916). Getling (1998) identifies the most important progress in the field. Most analyses have been undertaken for the idealized situation where the temperature is kept constant at the upper and lower fluid boundaries. This corresponds to the case of perfectly conducting slabs. However, most convection problems relevant to some engineering and geophysical problems do not have well-conducting slabs.

Convection in a layer heated from below can be precisely controlled and measured in the laboratory. However, to our knowledge, only Le Gal, Pocheau & Croquette (1988) have observed squares at the onset of buoyancy-driven convection between poorly conducting rigid slabs of low thermal conductivity. In the present investigation, we will consider two independently chosen slabs, each of finite thickness and thermal conductivity. This is relevant for comparison to experiments, in particular,

when transparent materials are applied for the slabs, making visualization by the shadowgraph technique possible.

Early investigations of the linear stability of Rayleigh–Bénard convection between poorly conducting boundaries were conducted by Jeffreys (1926) and Hurle, Jakeman & Pike (1967). The classical case of constant temperatures at the fluid boundaries were solved by Pellew & Southwell (1940), and Nield (1968) investigated the combination of a finite upper slab and constant temperature at the lower fluid boundary. Some of the later weakly nonlinear investigations also included some few selected linear stability results: for cases of infinite thick slabs by Riahi (1985) and for the case of two symmetric slabs of half the thickness of the fluid layer by Proctor (1981).

The stability of weakly nonlinear rolls for the case of constant temperatures at the fluid boundaries was first solved by Schluter, Lortz & Busse (1965). The problem of small-amplitude convection in the limit of poorly conducting slabs was investigated by Busse & Riahi (1980) and by Proctor (1981). Riahi (1985) took into account finite conductivities of two infinitely thick slabs and calculated the stability regions of squares and rolls. Jenkins & Proctor (1984) were the first to consider finite slabs, restricting their investigation to the case of two symmetric identical slabs.

Newell & Whitehead (1969) and Segel (1969) derived the Ginzburg–Landau equation for the case of constant temperature at the fluid boundaries. They showed that the bandwidth of stable wavenumbers for the rolls is limited by the cross-roll, the Eckhaus and the zigzag instabilities. Hoyle (1993) was the first to discover the instabilities that narrow the bandwith of stable squares. She studied a simplification of Proctor's model, valid only in the limit of two insulating slabs, where the wavenumber was assumed to be a small parameter in the problem. She determined a zigzag instability and a truly three-dimensional instability, which she denoted 'the rectangular Eckhaus instability'. The nature of this instability is, however, quite different from the Eckhaus instability. It is truly three-dimensional, modifying both the Fourier modes of the squares, and the wavenumber of this disturbance points in the 45° direction between the two wave vectors of the squares. Thus, this instability will not appear as 'rectangular' in experiments. Therefore, we will here rather denote it the long wavelength cross-roll instability (LW-CR).

The governing equations are presented in § 2. A transformation between this problem and the problem where the upper and lower slabs are changed round is given in § 3. Linear stability results are provided in § 4. The pattern selection and numerical calculations of stability regions for rolls and squares are presented in § 5, where also some remarks are made about the heat transfer. A theoretical stability analysis of two coupled Ginzburg–Landau equations is performed in § 6 predicting the wavenumber restrictions of stable squares owing to long-wavelength cross-roll and zigzag disturbances. It is shown how the cross-roll disturbances also influence another solution of the Ginzburg–Landau equations, the undulated rolls by Zaks *et al.* (1996). Summary and conclusions are made in § 7.

2. Governing equations

We consider a fluid layer of infinite horizontal extent and of constant depth h. The thermal conductivity k and the thermal diffusivity κ are constant properties. The coefficient of thermal expansion β describes the linear density dependence on temperature. The fluid is bounded by two rigid heat-conducting slabs. The upper slab has a thickness denoted by $h^{(u)}$, a thermal conductivity $k^{(u)}$ and a thermal diffusivity

$\kappa^{(u)}$. The corresponding quantities for the lower slab are denoted by $h^{(l)}$, $k^{(l)}$ and $\kappa^{(l)}$. Here and in what follows, the superscripts (u) and (l) refer to the upper and lower slabs.

The fluid is heated from below and cooled from above. The temperature is fixed at the outer boundaries of the slabs, and the temperature difference between these two boundaries is ΔT (positive). To describe the geometry and the flow, Cartesian coordinates (x, y, z) are used. The z-axis is directed upwards, with the origin located at the centre of the fluid layer. In the governing equations, the density is regarded as constant except in the buoyancy term (the Boussinesq approximation).

A temperature perturbation θ, a pressure perturbation p and a fluid motion $\boldsymbol{v}$ of the hydrostatic solution is considered. The corresponding temperature perturbations in the slabs are denoted $\theta^{(l)}$ and $\theta^{(u)}$. The dimensionless perturbation equations take the form

$$\nabla^2 \boldsymbol{v} + Ra\,\theta \boldsymbol{z} - \nabla p = Pr^{-1}\left(\frac{\partial \boldsymbol{v}}{\partial t} + \boldsymbol{v}\cdot\nabla\boldsymbol{v}\right), \tag{2.1}$$

$$\nabla^2\theta + \boldsymbol{v}\cdot\boldsymbol{z} = \frac{\partial\theta}{\partial t} + \boldsymbol{v}\cdot\nabla\theta, \tag{2.2}$$

$$\nabla\cdot\boldsymbol{v} = 0, \tag{2.3}$$

$$\nabla^2\theta^{(l)} = \frac{\kappa}{\kappa^{(l)}}\frac{\partial\theta^{(l)}}{\partial t}, \tag{2.4}$$

$$\nabla^2\theta^{(u)} = \frac{\kappa}{\kappa^{(u)}}\frac{\partial\theta^{(u)}}{\partial t}, \tag{2.5}$$

with boundary conditions

$$z = -\tfrac{1}{2} - H^{(l)}, \quad \tfrac{1}{2} + H^{(u)}: \quad \theta^{(l,u)} = 0, \tag{2.6}$$

$$z = -\tfrac{1}{2}, \quad \tfrac{1}{2}: \quad \boldsymbol{v} = 0, \quad \theta = \theta^{(l,u)}, \quad \frac{\partial\theta}{\partial z} = K^{(l,u)}\frac{\partial\theta^{(l,u)}}{\partial z}, \tag{2.7}$$

where the following thickness and conductivity ratios have been introduced:

$$H^{(l,u)} = h^{(l,u)}/h, \quad K^{(l,u)} = k^{(l,u)}/k. \tag{2.8}$$

Here, $\boldsymbol{z}$ is the vertical unit vector. Equations (2.1)–(2.7) for the perturbation of the hydrostatic solution ($\boldsymbol{v}=0$ and $T - T(z=0) = -z$) have been made dimensionless using the scales h, h^2/κ, κ/h and $\kappa\nu\rho_0/h^2$ as units of length, time, velocity and pressure, respectively. As the temperature scale, the temperature difference between the top and the bottom of the fluid layer in the basic hydrostatic solution is applied.

$$\Delta T^{(f)} = \frac{\Delta T}{1 + H^{(u)}/K^{(u)} + H^{(l)}/K^{(l)}}. \tag{2.9}$$

Pr and Ra are the Prandtl number and the Rayleigh number, defined by

$$Pr = \frac{\nu}{\kappa}, \quad Ra = \frac{g\beta\Delta T^{(f)}h^3}{\kappa\nu}. \tag{2.10}$$

For the special case of symmetric slabs, our definition of Ra is equal to the one by Jenkins & Proctor (1984). The Rayleigh number is proportional to the overall temperature difference ΔT through the expression for $\Delta T^{(f)}$, as defined in (2.9).

3. A symmetry of the problem

We will here prove an important symmetry of the mathematical solution. Consider a dual configuration, which differs from the first one in that the upper slab is placed below the fluid layer and the lower slab is placed above. The mathematical solution of this new problem follows by a transformation of the solution of the first problem, including the temperature variation in the two slabs. By applying the transformation

$$\left(u, v, w, \theta, p, \theta^{(l)}, \theta^{(u)}, z\right) \rightarrow \left(u, v, -w, -\theta, p, -\theta^{(l)}, -\theta^{(u)}, -z\right), \tag{3.1}$$

to the problem, defined by (2.1)–(2.7), we obtain exactly the same equation system, except that the upper and lower slabs are exchanged. This gives the important result that the mean heat transfer and the preferred flow pattern would be the same in an experiment where the equipment is turned upside down. For the special case of two symmetric slabs, it follows that the upward directed flow is mirrored by the downward directed flow.

4. Linear stability

It can easily be shown that the system (2.1)–(2.7) is self-adjoint. Hence, the time derivative vanishes at the onset of convection. With no loss of generality, the linear stability problem can be solved by assuming an eigen mode of the form $\theta = \hat{\theta}(z)\exp(\mathrm{i}\alpha x)$, where the α is the wavenumber (correspondingly for $\boldsymbol{v}$, p and $\theta^{(l,u)}$). The critical Rayleigh number, Ra_c, and the critical wavenumber, α_c, then depend only on the four slab properties $H^{(l,u)}$ and $K^{(l,u)}$.

In order to give a compact presentation of our results, we introduce two new dimensionless parameters that might be regarded as the effective conductivities of the slabs:

$$\xi^{(l,u)} = \begin{cases} K^{(l,u)}/H^{(l,u)} & \text{if } H^{(l,u)} \leqslant 1, \\ K^{(l,u)} & \text{if } H^{(l,u)} > 1. \end{cases} \tag{4.1}$$

Figure 1(*a–d*) shows Ra_c as a function of the slab properties $\xi^{(l,u)}$ for the cases when the slab thicknesses are comparable to the thickness of the fluid layer, i.e. when $0.1 \leqslant H^{(l,u)} \leqslant 1$. In figure 1(*e*) Ra_c is shown as a function of $\xi^{(l)}$ and $\xi^{(u)}$ for all combinations of infinitely thick or thin slabs. Figure 1(*f*) indicates the critical wavenumbers corresponding to the cases in figure 1(*e*). These asymptotic cases in figure 1(*e*, *f*) are close approximations when $H^{(l,u)} > 1$ or $H^{(l,u)} < 0.1$.

We note from figure 1(*e,f*) that the commonly applied approximation of perfectly conducting slabs, $Ra_c = 1707.8$ and $\alpha_c = 3.12$ by Pellew & Southwell (1940), is valid only when $\xi^{(l,u)}$ are rather large, in the range 10–100. At the other extreme, the case of insulating slabs, $Ra_c = 720$ and $\alpha_c = 0$ by Jeffreys (1926), is unrealistic to attain experimentally, because of the small wavenumbers involved.

Our results in figure 1(*a–d*) are relevant for the experimental conditions, covering the entire range of thicknesses and conductivities of two arbitrarily chosen finite slabs. Note that the use of $\xi^{(l,u)}$ roughly takes into account the influence of the slab thicknesses. Hence, the results in the limits of thin or thick slabs in figure 1(*e,f*) provide fairly good estimates even for the cases with finite slabs in figure 1(*a–d*).

5. The pattern selection

The existence of an extremum principle for weakly nonlinear convection was derived by Busse (1967). In this section, we will reduce the governing equations of the

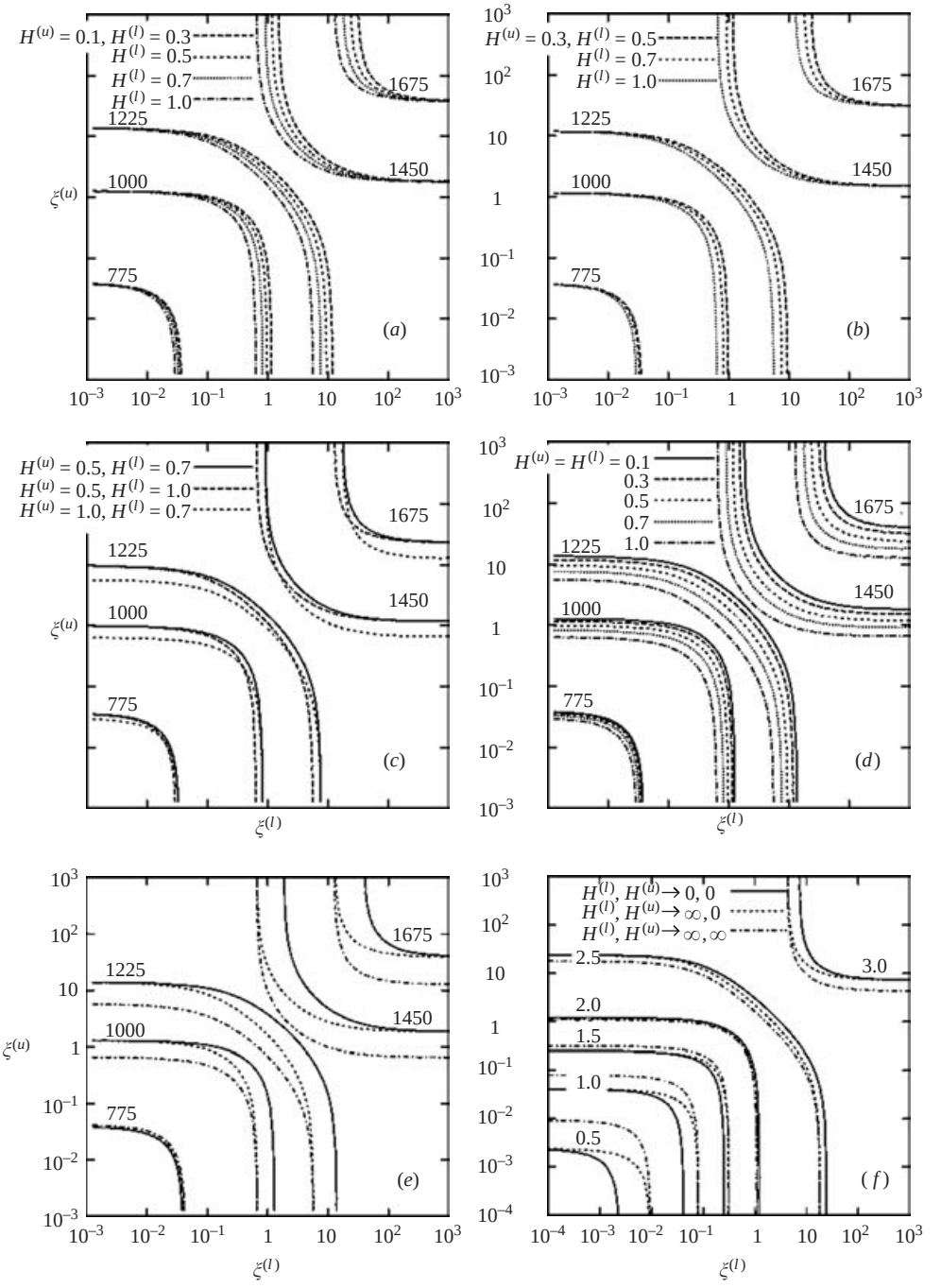

FIGURE 1. (*a*)–(*d*) The dependency of Ra_c on the effective conductivities of the slabs, $\xi^{(l)}$ and $\xi^{(u)}$, for the indicated combinations of slab thicknesses. (*e*) The dependency of Ra_c on the effective conductivities of the slabs, $\xi^{(l)}$ and $\xi^{(u)}$, for the possible combinations of infinitely thick and thin slabs. (*f*) The dependency of α_c on the effective conductivities of the slabs, $\xi^{(l)}$ and $\xi^{(u)}$, for the possible combinations of infinitely thick and thin slabs.

problem to an infinite set of coupled Landau equations, and then apply a maximum principle to determine which planforms are stable. By the use of the limiting case of two insulating slabs as a lower bound, we will prove that all solutions are unstable except either rolls or rhombuses. Our analysis of the Landau equations is comparable to the one by Malomed, Nepomnyashchy & Tribelsky (1989). However, our analysis is more general and complete in the sense that we include an infinite number of randomly oriented wave vectors, whereas their work was restricted to up to six evenly distributed wave vectors.

For supercritical Rayleigh numbers near the onset of convection, a weakly nonlinear expansion can be made.

$$\theta = \epsilon\theta^{(1)} + \epsilon^2\theta^{(2)} + \cdots, \tag{5.1}$$

where

$$\theta^{(1)} = \hat{\theta}(z)\sum_{n=1}^{N} A_n \exp(\mathrm{i}\boldsymbol{\alpha}_n \cdot \boldsymbol{r}) + \text{c.c.} \tag{5.2}$$

Here, c.c. denotes the complex conjugate terms, $|\boldsymbol{\alpha}_n| = \alpha_c$ and $\boldsymbol{r} = (x, y)$. The mathematical details of this expansion are omitted here, since similar techniques have been applied in previous works (for a review see Getling 1998). Further details are also given in Holmedal (1998). The result is that the governing equations (2.1)–(2.7) are reduced to a system of coupled Landau equations:

$$\frac{\mathrm{d}C_n}{\mathrm{d}t} = \epsilon C_n - C_n^3 - \sum_{\substack{m=1 \\ n\neq m}}^{N} \beta_{mn} C_m^2 C_n. \tag{5.3}$$

Here, the amplitudes $C_n \propto \epsilon A_n$, and the reduced Rayleigh number ϵ is assumed to be a small quantity,

$$\epsilon = \frac{Ra - Ra_c}{Ra_c}. \tag{5.4}$$

The coupling coefficients β_{mn} are real-valued parameters that depend on the angle, ϑ_{mn}, between the wave vectors $\boldsymbol{\alpha}_m$ and $\boldsymbol{\alpha}_n$. Since here all the coefficients of the Landau equations are real-valued, we have, in (5.3), without loss of generality, chosen the amplitudes C_n to be real-valued.

Figure 2 displays β_{mn} as a function of ϑ_{mn} for some selected sets of the external parameters. For the sake of simplicity, the subscripts of β and ϑ will be omitted when this is convenient. For any given value of ϑ, we have found that β is a minimum when both slabs are insulating (curve *e*). We note the general result that $\beta = 2$ for vanishing value of ϑ (for all types of slabs). Since $\beta > 0$ for all types of slabs and values of ϑ, the onset of convection occurs as a forward bifurcation and no sub-critical motions are possible. The limit of two insulating slabs and an infinite Prandtl number has been investigated by Busse & Riahi (1980). This limit yields the curve labelled *e* in the figure. Its analytical formula is:

$$\beta_{\mathrm{e}}(\vartheta) = \tfrac{2}{3}(1 + 2\cos^2\vartheta). \tag{5.5}$$

In the Appendix, we use this curve (5.5) as a lower bound for an extremum principle of the Landau equations (5.3) to prove that when $\beta(\pi/2) > 1$ only rolls are stable, whereas only rhombuses are stable when $\beta(\pi/2) < 1$. All quasi-periodic structures involving higher numbers of modes are proved to be unstable. Our results are in agreement with the analysis by Malomed *et al.* (1989). It should be mentioned that

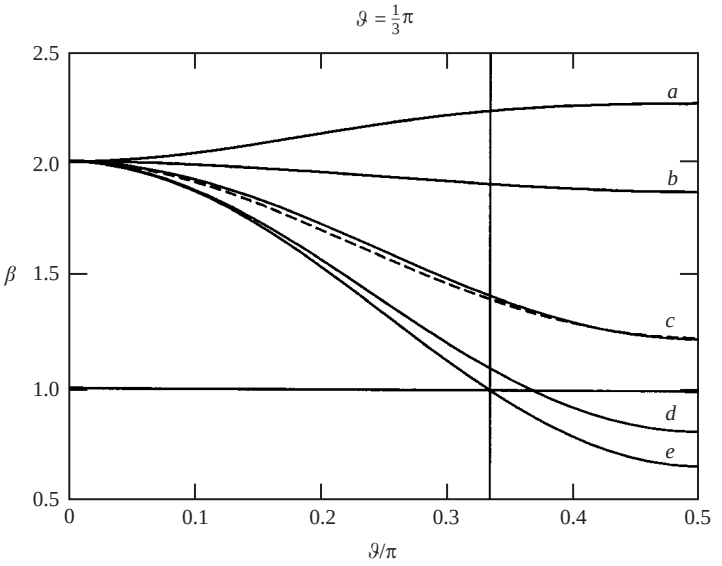

FIGURE 2. The Landau coefficient β as a function of the angle ϑ between the wave vectors. (*a*) One slab insulating, the other slab perfectly conducting and $Pr = 0.2$. (*b*) Two symmetric slabs with $(K^{(l,u)}, H^{(l,u)}) = (0.1, 1)$ and $Pr = 0.1$. (*c*) Both slabs perfectly conducting (solid line) and one slab insulating and the other slab perfectly conducting (dashed line) for cases of infinite Pr. (*d*) $(K^{(l)}, H^{(l)}) = (0.05, 0.5)$, $(K^{(u)}, H^{(u)}) = (0.1, 1)$ and infinite Pr. (*e*) Both slabs insulating and infinite Pr.

Rucklidge & Rucklidge (2003) questioned the reliability of calculating the properties of the quasi-patterns by the use of Landau equations.

It can be shown that $Nu_{rhombuses} - 1 = 2(Nu_{rolls} - 1)/(1 + \beta(\vartheta_{rhombuses}))$, where $Nu = 1 + (\mathrm{d}\overline{\theta}/\mathrm{d}z)_{z=-1/2}$ is the Nusselt number, where the overbar denotes the horizontal average. Hence, the solution that is stable has the strongest heat transport through the fluid layer. Squares, which are rhombuses with orthogonal wave vectors, have the largest growth rate and the strongest heat transport when two-mode solutions are stable.

The initial slope of the heat transport curve, $\mathrm{d}Nu/\mathrm{d}\epsilon$, vanishes in the limit where at least one of the slabs is insulating or infinitely thick. A comment should be made here about the works by Busse & Riahi (1980) and Riahi (1985). Their Nusselt and Rayleigh numbers are based on the temperature difference between the mean temperatures at the fluid boundaries. This temperature scale depends on the realized flow and is not proportional to the externally forced ΔT. Therefore, the initial slope of the heat transport curve based on their temperature scale remains finite in the insulating limit.

5.1. *Numerical stability results*

We have proved that the only possible stable pattern is either rolls or rhombuses, and that these solutions mutually exclude each other. We will now present the results from numerical calculations, where for given $K^{(l,u)}$, $H^{(l,u)}$ and Pr, the value of $\beta(\pi/2)$ has been calculated to determine whether rolls or rhombuses are stable.

It is interesting to consider the stability of the experiment by Le Gal, Pocheau & Croquette (1988). They carried out their experiment using Plexiglas and water, the parameters being $K^{(l)} = K^{(u)} = 0.4$, $H^{(l)} = H^{(u)} = 2$ and $Pr = 7$. For the observed squares, they estimated the wavenumber to be $\alpha = 2.5$. According to our linear

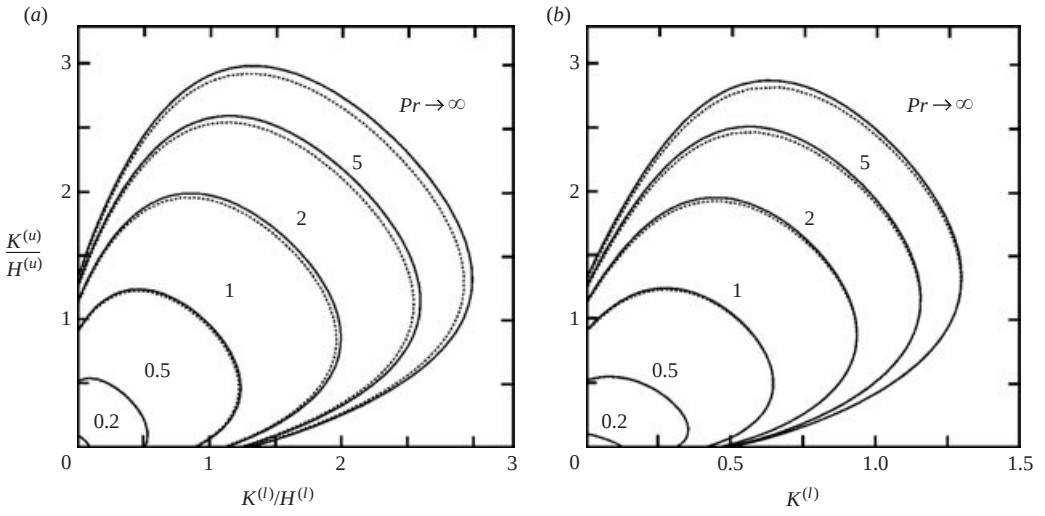

FIGURE 3. Regions of stable rhombuses. (*a*) In the $(K^{(l)}/H^{(l)}, K^{(u)}/H^{(u)})$-plane for various Prandtl numbers when both slabs are infinitely thin. (*b*) In the $(K^{(l)}, K^{(u)}/H^{(u)})$-plane for various Prandtl numbers when the lower slab is infinitely thick and the upper slab infinitely thin. The dotted curves denote the same stability curves, but with $H^{(l)} = 1$ and $H^{(u)} = 0.1$. Rolls are stable outside the regions.

results, the critical point for their set-up is $(\alpha_c, Ra_c) = (1.96, 1072)$. Using this critical wavenumber instead of their estimate, we find $\beta(\pi/2) = 0.92$, for which squares indeed are stable. Applying their wavenumber estimate yields $\beta(\pi/2) = 0.96$, also stable.

The stability curves depend on only one slab parameter, $K^{(l,u)}/H^{(l,u)}$, for slabs that are sufficiently thin. The stability curves for the limit of two infinitely thin slabs are displayed in figure 3(*a*) for selected values of the Prandtl number. The dotted lines indicate the case of two slabs having one-tenth of the thickness of the fluid layer.

The stability curves depend only on $K^{(l,u)}$, for slabs that are sufficiently thick. Figure 3(*b*) shows stability results in the limit of one infinitely thick and one infinitely thin slab for a selection of Prandtl numbers. The dotted lines show approximately the same results for the case where the thin slab is one-tenth as thick as the fluid layer, and the thick slab is equally thick as the fluid layer. The results in figure 3 suggest that if a slab is thinner than one-tenth of the fluid layer or thicker than the layer, the stability curves are approximately equal as if the slab was infinitely thin or thick, respectively.

Finally, in figure 4, we display the stability curves with $Pr \to \infty$, for finite values of $H^{(l)}$ and $H^{(u)}$. Combinations of $H^{(l)}$ and $H^{(u)}$ with values 0.1, 0.3, 0.5, 0.7 and 1 are shown (remember, the two slabs may be exchanged without altering the stability results). These thicknesses are typical in experiments. The same kind of dependence on the thicknesses of the slabs, as shown in figure 4, is expected for other values of the Prandtl number.

6. The wavenumber selection

In the limit of small wavenumbers, the wavenumber selection of squares has been investigated by Hoyle (1993). Her starting point was Proctor's equation, valid in the limit of poorly conducting slabs where the wavenumber becomes very small. She was the first to show that the squares become unstable to the zigzag instability and a

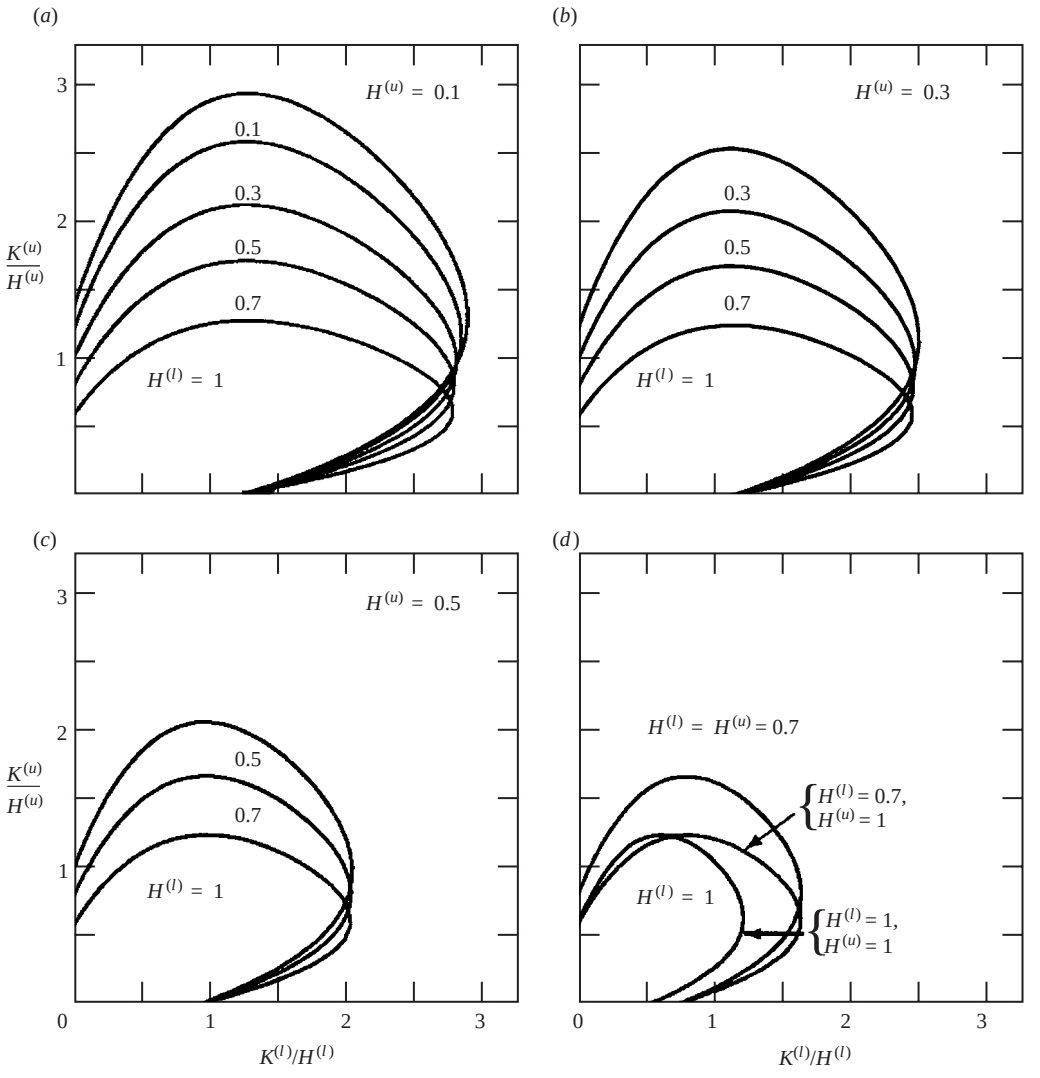

FIGURE 4. Regions of stable rhombuses in the $(K^{(l)}/H^{(l)}, K^{(u)}/H^{(u)})$-plane for infinite Prandtl number. Combinations of five selected thicknesses of the slabs in the range $0.1 \leqslant H^{(l,u)} \leqslant 1$ are shown. Rolls are stable outside the regions. Note that the upper and lower slab can be interchanged.

long-wavelength cross-roll instability. We will here consider the more general cases involving slabs of finite thicknesses and conductivities and finite wavenumbers. Our starting point will be a set of two coupled Ginzburg–Landau equations, which can be derived directly from the governing equations in a similar manner to the Landau equations, (5.2), but where, in addition, the amplitudes are allowed to vary slowly in the horizontal directions. To keep the algebra simple we will restrict our attention to squares, which is the special case of rhombuses that has the strongest growth.

$$\frac{\partial A}{\partial t} = \epsilon A + \frac{1}{2Ra_c}\frac{\mathrm{d}^2 Ra_c}{\mathrm{d}\alpha^2}\left(\frac{\partial}{\partial x} + \frac{1}{2\mathrm{i}\alpha_c}\frac{\partial^2}{\partial y^2}\right)^2 A - (|A|^2 + \beta|B|^2)A, \tag{6.1}$$

$$\frac{\partial B}{\partial t} = \epsilon B + \frac{1}{2Ra_c}\frac{\mathrm{d}^2 Ra_c}{\mathrm{d}\alpha^2}\left(\frac{\partial}{\partial y} + \frac{1}{2\mathrm{i}\alpha_c}\frac{\partial^2}{\partial x^2}\right)^2 B - (|B|^2 + \beta|A|^2)B, \tag{6.2}$$

here, $\beta = \beta(\pi/2)$.

We will now study the stability of squares with wavenumber near α_c. A stationary solution in the form of squares may be written

$$A = \sqrt{\frac{\epsilon - \epsilon_0}{1+\beta}}\,\exp(\mathrm{i}(\alpha - \alpha_c)x), \qquad B = \sqrt{\frac{\epsilon - \epsilon_0}{1+\beta}}\,\exp(\mathrm{i}(\alpha - \alpha_c)y), \tag{6.3}$$

where the reduced Rayleigh number on the neutral curve is

$$\epsilon_0 = \frac{1}{2Ra_c}\frac{\mathrm{d}^2 Ra_c}{\mathrm{d}\alpha^2}(\alpha - \alpha_c)^2. \tag{6.4}$$

Perturbations a and b of the amplitudes A and B yield solutions of the type:

$$a = (a_1\exp(\mathrm{i}qx + \mathrm{i}ry + \sigma t) + a_2^*\exp(-\mathrm{i}qx + \mathrm{i}ry + \sigma^* t))\exp(\mathrm{i}(\alpha - \alpha_c)x),$$
$$b = (b_1\exp(\mathrm{i}qx + \mathrm{i}ry + \sigma t) + b_2^*\exp(-\mathrm{i}qx + \mathrm{i}ry + \sigma^* t))\exp(\mathrm{i}(\alpha - \alpha_c)y),$$

where a_1, a_2, b_1 and b_2 are constants and $*$ denotes the complex conjugate. The characteristic fourth-order stability polynomial for the growth, σ, then can be written

$$D_{qr}D_{rq} - 4\beta^2(\sigma + X_{qr})(\sigma + X_{rq})(\epsilon - \epsilon_0)^2 = 0, \tag{6.5}$$

where

$$D_{qr} = (1+\beta)\left((\sigma + X_{qr})^2 - U_{qr}^2\right) + 2(\sigma + X_{qr})(\epsilon - \epsilon_0),$$
$$X_{qr} = \frac{1}{2Ra_c}\frac{\mathrm{d}^2 Ra_c}{\mathrm{d}\alpha^2}\left(\frac{r^4}{4\alpha_c^2} + q^2 + (\alpha - \alpha_c)\frac{r^2}{\alpha_c}\right),$$
$$U_{qr} = \frac{1}{2Ra_c}\frac{\mathrm{d}^2 Ra_c}{\mathrm{d}\alpha^2}\left(2(\alpha - \alpha_c) + \frac{r^2}{\alpha_c}\right)q.$$

In general, the four roots, σ, must be found numerically. However, we have derived analytically the two roots causing the fast-growing disturbances. For the special case with $|q| = |r| = s$, one of the roots of (6.5) is

$$\sigma = -\frac{(\epsilon - \epsilon_0)(1-\beta)}{(1+\beta)} + \sqrt{\frac{(\epsilon - \epsilon_0)^2(1-\beta)^2}{(1+\beta)^2} + U_{ss}^2} - X_{ss}. \tag{6.6}$$

For small values of s and close to the critical point we find

$$\sigma = \frac{s^2}{2Ra_c}\frac{\mathrm{d}^2 Ra_c}{\mathrm{d}\alpha^2}\left(\frac{3+\beta}{1-\beta}\frac{\epsilon_0}{\epsilon} - 1\right) + O(s^4, (\alpha - \alpha_c)^3 s^2). \tag{6.7}$$

Therefore, a necessary condition for the stability of squares is that

$$\epsilon > \frac{3+\beta}{1-\beta}\epsilon_0. \tag{6.8}$$

The eigenvector of this disturbance is

$$(a_1, a_2, b_1, b_2) = (\overline{a}, \overline{b}, -\overline{a}, -\overline{b}), \tag{6.9}$$

where $\overline{a} = -(\epsilon - \epsilon_0)(1-\beta)/(1+\beta)$ and $\overline{b} = \sqrt{(\epsilon - \epsilon_0)^2(1-\beta)^2/(1+\beta)^2 + U_{ss}^2} + U_{ss}$. Since the signs of the disturbances a and b are opposite, one of the two rolls will grow

locally at the expense of the other. Clearly, this instability is the long-wavelength cross-roll instability (LW-CR), that Hoyle (1993) denoted 'the rectangular Eckhaus instability'.

The other important instability is found with either $(q, r) = (0, s)$ or $(q, r) = (s, 0)$. One of the roots of (6.5) is then easily obtained as

$$\sigma = -\frac{s^2}{2\alpha_c Ra_c}\frac{\mathrm{d}^2 Ra_c}{\mathrm{d}\alpha^2}(\alpha - \alpha_c) - \frac{s^4}{8\alpha_c^2 Ra_c}\frac{\mathrm{d}^2 Ra_c}{\mathrm{d}\alpha^2}, \tag{6.10}$$

This root causes an instability of the squares if

$$\alpha < \alpha_c. \tag{6.11}$$

This is similar to the condition for zigzag instability of the rolls. The eigenvector of this disturbance may be written

$$(a1, a2, b1, b2) = \begin{cases} (1, -1, 0, 0), & q = 0, r = s, \\ (0, 0, 1, -1), & q = s, r = 0. \end{cases} \tag{6.12}$$

We recognize this instability as the zigzag instability, a well-known instability for the case of rolls. Here, it affects independently each of the two crossed rolls that the squares consist of.

The stability region of the squares yields the same type of instability as first discovered for the limit of small wavenumbers and poorly conducting slabs by Hoyle (1993). It is reasonable to expect similar stability properties of rhombuses with $\vartheta \neq \pi/2$, by adopting $\beta = \beta(\vartheta)$ in (6.8) and (6.11).

For the case of rolls, the instabilities are well known: the zigzag instability for $\alpha < \alpha_c$; the Eckhaus instability for $\epsilon < 3\epsilon_0$; and the cross-roll instability for $\epsilon < \epsilon_0\beta/(\beta - 1)$. When $\beta > 1.5$, the Eckhaus instability is stricter than the cross-roll instability, which is the case for low Prandtl numbers.

Zaks *et al.* (1996) showed that undulated rolls can be a stable solution for wavenumbers that are smaller than the critical one. The undulated rolls can be expressed as the following approximate solution of (6.1) with $B = 0$ and:

$$A = A_{01}\exp(\mathrm{i}(\alpha - \alpha_c)x) + A_{02}\exp(\mathrm{i}(\alpha - \alpha_c)x + \mathrm{i}py) + A_{03}\exp(\mathrm{i}(\alpha - \alpha_c)x - \mathrm{i}py), \tag{6.13}$$

where

$$A_{02}^2 = A_{03}^2 = \frac{1}{Ra_c}\frac{\mathrm{d}^2 Ra_c}{\mathrm{d}\alpha^2}\left((\alpha - \alpha_c)^2 - \left(\alpha - \alpha_c + \frac{p^2}{2\alpha_c}\right)^2\right), \tag{6.14}$$

$$A_{01}^2 = \epsilon_c - \frac{1}{Ra_c}\frac{\mathrm{d}^2 Ra_c}{\mathrm{d}\alpha^2}\left(3(\alpha - \alpha_c)^2 - 2\left(\alpha - \alpha_c + \frac{p^2}{2\alpha_c}\right)^2\right). \tag{6.15}$$

Here, p denotes the transverse component of the wave vector. It can be extracted from their work that the undulated rolls are stable in the region where

$$5.828\epsilon_0 \leqslant \epsilon \leqslant 7\epsilon_0, \qquad \alpha < \alpha_c. \tag{6.16}$$

Zaks *et al.* (1996) did not include cross-roll disturbances in their analysis. It can be shown that the undulated rolls are unstable to a cross-roll instability when

$$\epsilon < \frac{\beta}{\beta - 1}\,\epsilon_0 - \frac{\mathrm{d}^2 Ra_c}{\mathrm{d}\alpha^2}\frac{p^2}{2Ra_c}\left(4(\alpha - \alpha_c) + \frac{p^2}{\alpha_c^2}\right). \tag{6.17}$$

It follows that all the undulated roll solutions are unstable when $\beta < 7/6$. Hence, the undulated rolls are only just stable for the case of large Prandtl numbers and

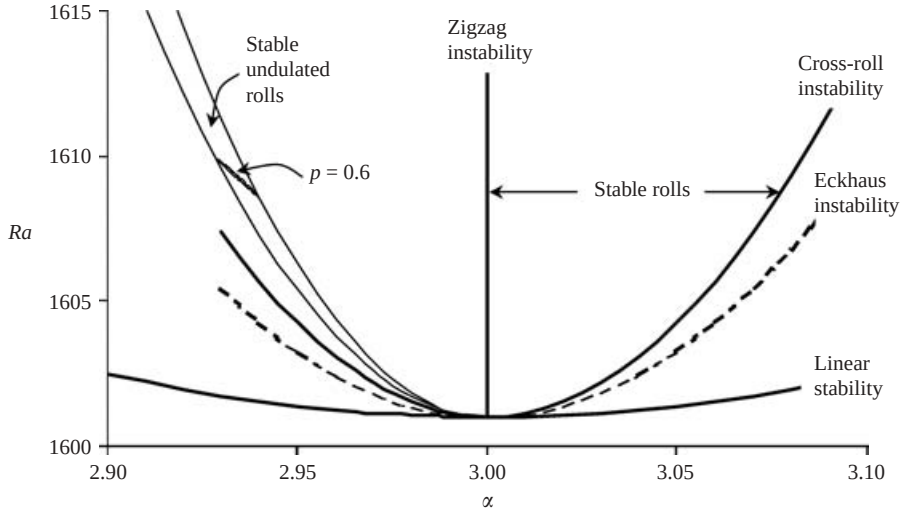

FIGURE 5. An example ($\alpha_c = 3$, $Ra_c = 1601$, $\partial^2 Ra_c/\partial\alpha^2 = 300$, $\beta = 1.3$) of stability regions of rolls and of undulated rolls. The stability of the rolls is restricted by the zigzag instability from the left-hand side and by the cross-roll instability from the right-hand side. The stable region of the undulated rolls contains solutions, where the wavenumber p of the variation along the roll axis increases with the distance from the critical point. The tiny stability region for one particular value, $p = 0.6$, is included.

well-conducting boundaries, for which $\beta \to 1.23$. Their stability is strengthened with decreased Pr, and also with increased $K^{(l,u)}/H^{(l,u)}$ in the general case.

An example of the stability regions of rolls and of undulated rolls is given in figure 5. A narrow wedge of stability is obtained for each value of p, the one obtained for $p = 0.6$ being included in the figure. In this example, $\beta < 1.5$ and therefore the stability region of the rolls is enclosed within the zigzag instability and the cross-roll instability.

Other stationary solutions involving a slow variation of the amplitudes are likely to exist also for rhombuses. However, this is beyond the scope of this investigation.

7. Summary and conclusions

We have investigated thermal convection in a horizontal fluid layer sandwiched between slabs of arbitrary thickness and thermal conductivity. A transformation has been found, which relates the solution for the case where the slabs are interchanged. This transformation is generally valid for the governing equations, within the Boussinesq approximation, giving the same type of nonlinear pattern and the same heat transfer when the slabs are interchanged.

The critical Rayleigh number for the onset of convection has been calculated as a function of the slab properties. The weakly nonlinear problem has been reduced to a set of coupled Landau equations by a weakly nonlinear expansion. A maximum principle of the Landau equations and the solution for the limit of insulating slabs has been applied to show that the only stable planform is either rolls or rhombuses. The stable solutions have the largest heat transfer through the fluid layer. We have calculated numerically which pattern is stable, depending on the slab properties and the Prandtl number.

The investigation of two coupled Ginzburg–Landau equations revealed that also for cases with finite thicknesses and conductivities of the slabs, the wavenumbers of stable squares are restricted by the instabilities first discovered by Hoyle (1993) for poorly conducting boundaries and small wavenumbers. These are the zigzag instability and a long-wavelength cross-roll instability. Furthermore, we have shown that the undulated rolls by Zaks *et al.* (1996) have a smaller stability region than the rolls as a function of the slab properties, because of restrictions on the allowed wavenumbers by the cross-roll instability.

A couple of interesting questions arise from this work. First, do stable 'undulated rhombuses' exist? i.e. a two-mode version of the undulated rolls with amplitudes that vary slowly in the horizontal directions. Secondly, what happens near the stability border between rolls and rhombuses? The stability of fully nonlinear solutions for squares and rolls is by Holmedal (2005).

Appendix. Stability of the Landau equations

In order to discuss the stability of stationary solutions of the Landau equations, (5.3), we apply their potential V:

$$V = \tfrac{1}{2}\epsilon \sum_n C_n^2 - \tfrac{1}{4}\sum_n C_n^4 - \tfrac{1}{4}\sum_{\substack{mn \\ m\neq n}} \beta_{mn} C_m^2 C_n^2. \tag{A 1}$$

The Landau equations, (5.3), can then be written as

$$\frac{\mathrm{d}C_n}{\mathrm{d}t} = \frac{\partial V}{\partial C_n}, \tag{A 2}$$

from which it follows that the N-dimensional vector $\mathrm{d}C_n$ is always directed towards increasing value of V. The function V will therefore continuously increase until it eventually attains a maximal value corresponding to a stable steady solution.

For any stationary solution we must have

$$\frac{\partial V}{\partial C_n} = 0, \quad n = 1, \ldots, N. \tag{A 3}$$

Furthermore, to ensure that the stationary solution corresponds to a maximum point (stable solution), the matrix $-\partial^2 V/\partial C_i \partial C_j = -V_{ij}$, must be positive definite. A necessary and sufficient condition for positive definiteness is that the leading principal minor determinants

$$H_n = \det \begin{pmatrix} V_{11} & V_{12} & \cdots & V_{1n} \\ V_{21} & V_{22} & \cdots & V_{2n} \\ \vdots & & & \vdots \\ V_{n1} & V_{n2} & \cdots & V_{nn} \end{pmatrix} (-1)^n \quad (n \leqslant N), \tag{A 4}$$

are positive, i.e. $H_1 > 0$, $H_2 > 0, \ldots,$ $H_n > 0$.

The signs of the determinants H_n are determined by the values of the Landau coefficients β_{mn}. We therefore begin the stability analysis by noting that because of the rotational symmetry of the problem, it is easy to show that the function $\beta(\vartheta_{mn})$ is symmetric about $0, \pi/2, \pi, \ldots$.

A.1. *Stability of one-mode solutions (rolls)*

Let us consider the solution of the Landau equations, (5.3), with one non-zero amplitude only: $C_1^2 = \epsilon$, $C_j = 0$, $j \neq 1$. This steady solution represents rolls. The leading principal minor determinant of order n then becomes

$$H_n = 2\epsilon^n(\beta_{12} - 1)(\beta_{13} - 1)\cdot\cdots\cdot(\beta_{1n} - 1). \tag{A 5}$$

We conclude that a necessary and sufficient condition for the roll solution to be stable is that

$$\beta(\vartheta) > 1 \quad \text{for all} \quad \vartheta \in [0, \pi/2]\,. \tag{A 6}$$

A.2. *Stability of two mode solutions (rhombuses)*

An arbitrary two-mode solution of the Landau equations is given by $C_1^2 = C_2^2 = \epsilon/(1+\beta_{12})$ and $C_j = 0$ when $j > 2$. From (A 4), we obtain the leading principal minor determinants:

$$H_1 = \frac{2\epsilon}{1+\beta_{12}}, \qquad H_2 = 4\epsilon(1-\beta_{12}), \tag{A 7}$$

$$H_n = H_2\epsilon^{n-2}\left(\frac{\beta_{13}+\beta_{23}-1-\beta_{12}}{1+\beta_{12}}\right)\left(\frac{\beta_{14}+\beta_{24}-1-\beta_{12}}{1+\beta_{12}}\right) \cdots \left(\frac{\beta_{1n}+\beta_{2n}-1-\beta_{12}}{1+\beta_{12}}\right), \qquad n = 3, 4, \ldots. \tag{A 8}$$

Here, β_{1n} and β_{2n} are the Landau coefficients which couple the solution modes to mode number $n = 3, 4, \ldots$. The solution is stable if, and only if, all H_n are positive. Hence, to ensure that the solution is stable, we must have fulfilled the conditions

$$\beta_{12} < 1, \tag{A 9}$$

$$\beta_{1n} + \beta_{2n} > 1 + \beta_{12} \quad (n = 3, 4, \ldots). \tag{A 10}$$

We will now show that the condition (A 10) is always fulfilled if condition (A 9) holds. Let us consider a mode number 3 (not part of the stationary solution). If condition (A 9) is fulfilled, then condition (A 10) is satisfied if

$$\beta_{13} + \beta_{23} \geqslant 2. \tag{A 11}$$

Condition (A 11) replaces condition (A 9) since mode 3 is chosen arbitrarily. We will use $\beta > \beta_e$, where $\beta_e = \left(1 + 2\cos^2\vartheta\right)2/3$, as a lower limit for the right-hand side of the inequality (A 11):

$$\beta_{13} + \beta_{23} \geqslant \beta_{\mathrm{e}}(\vartheta_{13}) + \beta_{\mathrm{e}}(\vartheta_{23}). \tag{A 12}$$

From the constraint $\beta > \beta_e$, it follows that in the search for stable solutions it is sufficient to consider ϑ_{12} in the interval

$$\vartheta_{12} \in \left\langle \tfrac{1}{3}\pi,\ \tfrac{2}{3}\pi\right] . \tag{A 13}$$

Let us apply the symmetries of β and rewrite the right-hand side of inequality (A 12):

$$\begin{aligned}\beta_{\mathrm{e}}(\vartheta_{13}) + \beta_{\mathrm{e}}(\vartheta_{23}) &= \beta_{\mathrm{e}}(\vartheta_{13}) + \beta_{\mathrm{e}}(\vartheta_{13} - \vartheta_{12}) \\ &= \tfrac{4}{3}(1 + \cos^2\vartheta_{13} + \cos^2(\vartheta_{13} - \vartheta_{12})).\end{aligned} \tag{A 14}$$

A straightforward analysis of this expression gives

$$\beta_{\mathrm{e}}(\vartheta_{13}) + \beta_{\mathrm{e}}(\vartheta_{23}) > 2 \quad \text{for} \quad \vartheta_{12} \in \left\langle \tfrac{1}{3}\pi,\ \tfrac{2}{3}\pi\right] , \tag{A 15}$$

for any choice of ϑ_{13}. Hence, the condition (A 11) and thereby (A 10) is always fulfilled if (A 9) is satisfied.

We have shown that the condition (A 7) that $\beta_{12} < 1$, is a necessary and sufficient stability criterion for rhombuses to be stable, provided the lower bound $\beta > \beta_e$.

A.3. *Stability of solutions involving three or more modes*

Finally, we examine the stability of a stationary solution composed of three or more (non-zero) modes. Let C_1 and C_2 denote the amplitudes of two of these modes (of relative orientation ϑ_{12}). From (A 4), it follows that the leading principal minor determinant H_2 is given by

$$H_2 = 4C_1^2C_2^2(1-\beta_{12})(1+\beta_{12}). \tag{A 16}$$

We see that similarly as for the two-mode planform, instability occurs for $\beta_{12} > 1$. With the exception of pure hexagons, any planform involving three modes or more will always consist of modes where at least two of them have a relative orientation $\vartheta_{12} < \pi/3$. Since $\beta > \beta_e \geqslant 1$ always when $\vartheta_{12} \leqslant \pi/3$ it follows that all solutions involving three modes or more are unstable.

To investigate the singular case with $\beta = \beta_e$, higher-order terms must be added to the Landau equations. This limit represents a non-realistic theoretical limit for the case of Rayleigh–Bénard convection between finite slabs, and will therefore not be discussed further in this investigation.

REFERENCES

Bénard, H. 1900 Les Tourbillons cellulaires dans une nappe liquide. *Rev. Gén. Sci. Pure Appl.* **11**, 1309–1328.

Busse, F. H. 1967 The stability of finite amplitude cellular convection and its relation to an extremum principle. *J. Fluid Mech.* **30**, 625–649.

Busse, F. H. & Riahi, N. 1980 Nonlinear convection in a layer with nearly insulating boundaries. *J. Fluid Mech.* **96**, 243–256.

Getling, A. V. Rayleigh–Bénard Convection: Structures and Dynamics. *World Sceintific*.

Holmedal, B. 1998 Square and roll patterns in Rayleigh–Bénard convection with thermally conducting rigid boundaries. D Sci thesis, University of Oslo, Department of Mathematics, Mechanics Division, Norway.

Holmedal, B. 2005 Stability of squares and rolls in Rayleigh–Bénard convection in an infinite-Prandtl-number fluid between finite slabs. *J. Fluid Mech.* **537**, 271–284.

Hoyle, R. B. 1993 Long wavelength instabilities of square patterns. *Physica* D **67**, 198–223.

Hurle, D. T. J., Jakeman, E. & Pike, E. R. 1967 On the solution of the Bénard problem with boundaries of finite conductivity. *Proc. R. Soc. Lond.* A **296**, 469–475.

Jeffreys, H. 1926 The stability of a layer heated from below. *Phil. Mag.* **2**, 833–844.

Jenkins, D. R. & Proctor, M. R. E. 1984 The transition from roll to square-cell solutions in Rayleigh–Bénard convection. *J. Fluid Mech.* **139**, 461–471.

Le Gal, P., Pocheau, A. & Croquette, V. 1988 Appearance of a square pattern in a Rayleigh–Bénard experiment. *Phys. Fluids* **31**, 3440–3442.

Malomed, B. A., Nepomnyashchy, A. A. & Tribelsky, M. I. 1989 Two-dimensional quasiperiodic structures in nonequilibrium systems. *Sov. Phys. J. Exp. Theor. Phys.* **69**, 388–397.

Newell, A. C. & Whitehead, J. A. 1969 Finite bandwidth, finite amplitude convection *J. Fluid Mech.* **38**, 279–303.

Nield, D. A. 1968 The Rayleigh–Jeffreys problem with boundary slab of finite conductivity *J. Fluid Mech.* **32**, 393–398.

Pellew, A. & Southwell, R. V. 1940 On maintained convective motion in a fluid heated from below. *Proc. R. Soc. Lond.* A **176**, 312–343.

Proctor, M. R. E. 1981 Planform selection by finite-amplitude thermal convection between poorly conducting slabs. *J. Fluid Mech.* **113**, 469–485.

Rayleigh, Lord 1916 On convection currents in a horizontal layer of fluid when the higher temperature is on the under side. *Phil. Mag.* **32**, 529–546.

Riahi, N. 1985 Nonlinear thermal convection with finite conducting boundaries. *J. Fluid Mech.* **152**, 113–123.

Rucklidge, A. M. & Rucklidge, W. J. 2003 Convergence properties of the 8, 10 and 12 mode representations of quasipatterns. *Physica* D **178**, 62–82.

Schluter, A., Lortz, D. & Busse, F. 1965 On the stability of steady finite amplitude convection. *J. Fluid Mech.* **23**, 129–144.

Segel, L. A. 1969 Distant side-walls cause slow amplitude modulation of cellular convection. *J. Fluid Mech.* **38**, 203–224.

Zaks, M. A., Auer, M. & Busse, F. 1996 Undulated rolls and their instabilities in a Rayleigh–Bénard layer. *Phys. Rev.* E **53**, 4807–4819.